LiDAR Measurements of Wind Shear Exponents and Turbulence Intensity Offshore the Northeast United States

Anthony Viselli[1]
Advanced Structures and Composites Center,
University of Maine,
35 Flagstaff Road,
Orono, ME 04469
e-mail: anthony.viselli@maine.edu

Nathan Faessler
Advanced Structures and Composites Center,
University of Maine,
35 Flagstaff Road,
Orono, ME 04469
e-mail: nathan.faessler@maine.edu

Matthew Filippelli
UL,
463 New Karner Road,
Albany, NY 12205
e-mail: matthew.filippelli@ul.com

This paper presents wind speed shear exponents and turbulence intensity (TI) measurements collected from light imaging, detection, and ranging instruments (LiDARs) measuring wind speeds from 40 m to 200 m above sea level and provides comparisons to industry design guidelines. The high-altitude wind speed data are unique and represent some of the first measurements made offshore in this part of the country, which is actively being developed for offshore wind. The data are used to support the New England Aqua Ventus I Floating Offshore Wind Farm to be located 17 km offshore the Northeast United States. Multiple LiDAR measurements were made using a DeepCLiDAR floating buoy and LiDARs located on a nearby island. The measured wind speed shear exponents are compared against industry standard mesoscale model outputs and offshore design codes including the American Bureau of Shipping, American Petroleum Institute, and Det Norske Veritas-Germanischer Lloyd guides. Significant variation in the vertical wind speed profile occurs throughout the year which is not addressed in design standards. Additionally, TI measurements made from the LiDAR, although not widely accepted in the scientific community, are presented and compared against industry guidelines.
[DOI: 10.1115/1.4053583]

Keywords: offshore wind, LiDAR, ocean waves and associated statistics

1 Introduction

There is an increased need to characterize the high-altitude wind conditions offshore as wind energy is developed to meet the increasing renewable energy demand in the Northeast USA. Such measurement campaigns provide essential data to support project design activities while also generating unique measurements far-offshore. This paper presents some of the first US measurements of wind shear exponents and turbulence intensity (TI) collected in support of offshore wind development. The data were collected by a floating light imaging, detection, and ranging instrument (LiDAR) buoy, and a nearby land-based LiDAR, located 17 km offshore the coast of Maine in the Northeast United States. The measurements were taken near the site of the US Department of Energy Advanced Offshore Wind Technology Project called New England Aqua Ventus I. The data represent one of the first high-altitude datasets collected in the USA. Wind shear exponents and TI measurements made by the LiDAR devices are compared with published design guides for offshore wind turbines and differences are highlighted. These early offshore measurements provide useful insights into the behavior of the wind speed exponents far-offshore in the Northeast USA and will help, as more data become available from other projects, support increased understanding and aid improvement of design methods and standards.

The paper first presents theory and background information useful in the understanding of the presented data and post-processing methods. Additional background on other offshore measurements of wind speed is also discussed briefly. The measurement setup is then explained for both the LiDAR buoy and land-based LiDAR measurement programs. Next, the data are presented followed by comparisons to industry published values. Finally, the paper concludes with a discussion of the results.

2 Theory and Background

2.1 Theory and Representative Measurements of Wind Shear Exponents. A brief discussion of wind shear and how it is typically represented in offshore wind design codes are now presented. Wind shear is the natural variation of the wind speed with the height above the earth's surface due to a variety of physical processes. This variation in wind speed is often represented with a power law model defined as

$$u = u_r \left(\frac{z}{z_r}\right)^{\alpha} \tag{1}$$

where the variables are as defined in the nomenclature section at the end of this paper. The power law wind shear extrapolation method is often used for engineering design purposes and exponents are generally in the range of 0.1–0.2 although wider ranges are in use. However, it is well known that a variety of wind shear profiles are possible due at a site due to different boundary layer conditions as shown in Fig. 1. Two measurement heights (z) are needed to determine α from experimental data. Wind speed measurements (u), in meters per second, taken at 40 and 100 m were used in this study from the LiDAR measurements. An upper height of 100 m was chosen because it represents a hub-height of a 6 MW wind turbine originally proposed for the project. Forty meters were chosen because it offered the most available data out of the remaining measurement heights. This resulted in the power law being treated as such

$$u_{100\,\mathrm{m}} = u_{40\,\mathrm{m}} \left(\frac{100}{40}\right)^{\alpha} \tag{2}$$

[1]Corresponding author.

Contributed by the Ocean, Offshore, and Arctic Engineering Division of ASME for publication in the Journal of Offshore Mechanics and Arctic Engineering. Manuscript received March 1, 2019; final manuscript received January 9, 2022; published online February 18, 2022. Assoc. Editor: Lance Manuel.

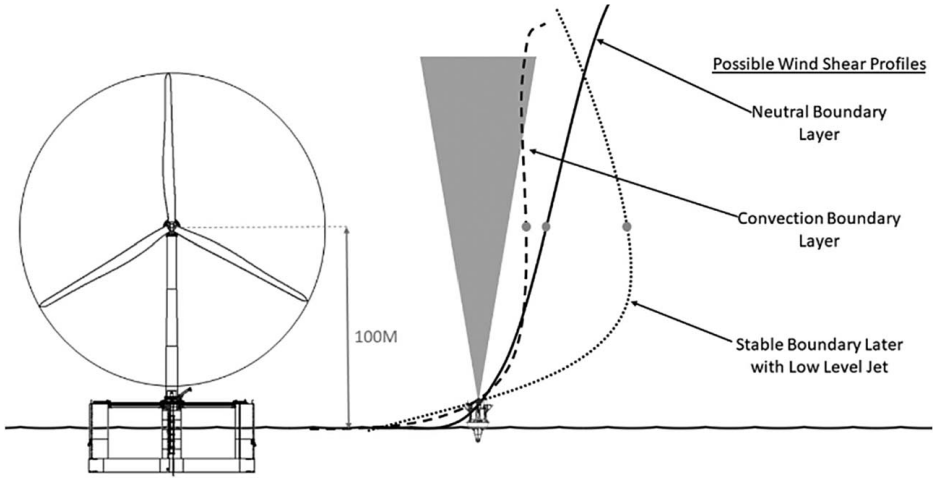

Fig. 1 Possible wind shear profiles offshore

Using the data and this relationship, the wind shear exponent could be solved for each measurement record.

A brief summary of known offshore wind measurements and wind shear exponents to provide context to the new measurements made in this study is now presented. Although there is a wealth of near surface data collected from oceanographic buoys in the USA, at this time there are few public datasets for offshore wind speed measurements at wind turbine hub heights (100+ m) available in the USA. The US Department of Energy launched a Wind Sentinel LiDAR buoy off the coast of Virginia in 2016 [1] and in Atlantic City, NJ. The National Renewable Energy Laboratory (NREL) has published US offshore wind resource maps, which present mean annual wind speeds at a height of 90 m. These plots have assumed an average wind shear exponent of 0.11 [2]. Similar studies of the great lakes have used shear coefficients of 0.10 in Lake Erie and Lake Ontario [3]. The University of Maine, with the use of metocean buoy data including surface level wind speed data and published mean wind speeds from NREL, estimated wind shear coefficients of 0.16 [4]. A short one-month campaign of ship mounted LiDAR measurements was performed off the coast of Maine in the summer of 2004 and showed a range of wind shear values between −0.02 and 0.06 [5].

In Europe, more published information on wind shear exists, likely due to the number of offshore wind farms currently installed. It has been shown that traditional methods for accounting for wind shear in the surface layer are often under estimated. It was observed by Bernhard Lange in 2004 that wind shear is often larger than predictions from traditional methods, especially in warmer air conditions [6]. This suggests that traditional methods may need to be modified where atmospheric stability is accounted for. Furthermore, the Technical University of Denmark (DTU) has performed studies in the North Sea using LiDAR devices and concluded that "current wind engineering commonly used wind shear norms and standards seem to be far too optimistic and not very conservative" [7]. The values from standards were generally lower than measurements. As such, these commonly used wind shear norms can lead to overestimation of long-term wind resource. Further studies performed by the DTU in the North Sea comparing wind shear measurements between met-masts and wind LiDARs show that the typically assigned offshore wind shear value of $\alpha = 0.2$ is only accurate for a very slim set of atmospheric and marine conditions [8]. Rather, it has been observed that wind shear values at 100 m have a range between −0.2 and 0.8.

Some design standards use a logarithmic wind shear model instead of the power law model. To compare the measured values to published values, equivalent wind shear power law exponents were calculated using Eq. (2.3.2.9) from the recommended practice from Det Norske Veritas-Germanischer Lloyd (DNV-GL), DNV-RP-C205 [9]:

$$\alpha = \frac{\ln((z/z_0)/(H/z_0))}{\ln(z/H)} \tag{3}$$

This equation is a combination of logarithmic and power law wind profiles and is height dependent. Here, H is equal to 40 m and z is equal to 100 m to be consistent with the power law wind shear exponent value calculation process. This equation allows a direct comparison of the two models for estimating variation of wind speed with height.

2.2 Theory and Representative Measurements of Wind Speed Turbulence Intensity. For the purposes of offshore wind turbine design, the wind speed TI is defined as the standard deviation (STD) of the wind velocity (u') over the mean wind velocity (u_{avg}) typically taken over a 10-min record of wind speeds sample with cup anemometers [10]:

$$\mathrm{TI} = \frac{u'}{u_{avg}} \tag{4}$$

Public wind TI measurements offshore in the USA at hub-height are also scarce. Europe has more data for wind turbulence, but most of these data are still proprietary. Two years of analyzed data are available from a costal measurement station in Norway. This analysis shows that offshore and costal environments tend to have a TI slightly less than the onshore sector. Furthermore, there is a distinct difference shown between seasons where the variations between these sectors are more pronounced in summer [11]. Multiple methods of predicting TI have been compared to measurements taken at the Greater Gabbard Offshore Wind Farm. This dataset shows mean TI values between 0.07 and 0.10 and between 3 and 25 m/s wind speeds, when taking into account all wind directions [12].

2.3 Summary of Offshore Wind Energy Design Values for Wind Shear Exponents and Turbulence Intensity From Industry Standards. Wind shear exponents recommended design values are provided in offshore engineering design guides. In this paper, a review of the published values was completed including:

- American Bureau of Shipping (ABS) Guide for Building and Classing Floating Offshore Wind Turbine Installations [13]

Table 1 Comparison of offshore wind shear exponents

Reference	ABS (operational/ extreme)	IEC 61400-3	DNV-RP-C205	ASCE
Wind shear exponent	0.11/0.14	0.20	0.12	0.15

- International Electrotechnical Commission (IEC) International Standard IEC 61400-3 [10]
- DNV-RP-C205 Environmental Conditions and Environmental Loads [9]
- American Society of Civil Engineers (ASCE) [14]

Table 1 presents a summary of the recommended wind shear exponents from these standards. The table shows that there is a significant difference between the standards for offshore wind designers. For example, the ABS guide differentiates between operational and extreme conditions while the other standards provide one value. The differences between the standards are significant. For example, a 5 m/s wind speed at 4 m above sea level, when extrapolated to 100 m hub-height using Eq. (1) and the published wind shear exponents, yields a wide range of wind speeds of 7.1, 9.5, 7.4, and 8.1 m/s for the four standards listed in the order presented in Table 1.

Wind turbine design conditions, including wind shear and wind veer, are given by IEC 61400-1. ABS references this same set of conditions. The IEC models are based on 90% quantile turbulence measurement and provide TI as a function of wind speed for the purposes of load calculation and to provide conservative estimates for design of offshore wind systems.

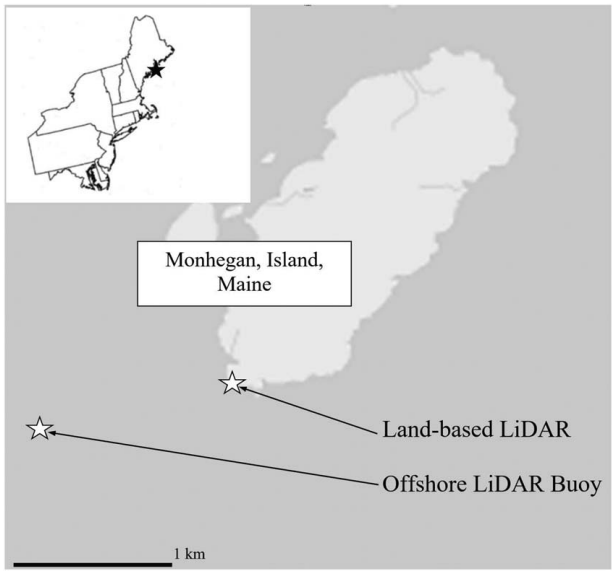

Fig. 2 LiDAR deployment test sites

3 Experimental Methods

3.1 LiDAR Measurements. Data were collected from a LiDAR on Monhegan Island and from a buoy approximately 1 km west of the Island as shown in Fig. 2. Monhegan Island itself is roughly 17 km from the mainland. The instruments and data collected are summarized in Table 2. Both LiDARs were Windcubes produced by Leosphere. The offshore measurements were collected using a Windcube V2 Offshore LiDAR, while the land-based data are comprised of measurements from both a Windcube V2 Offshore LiDAR and a Windcube V1 LiDAR deployed at different times. The V2 LiDAR is the next iteration of the V1 LiDAR and there are no significant difference in the data between the units after completing side-by-side comparisons on land and offshore as described by Viselli et al. [15]. The V2 Offshore LiDAR includes built in motion correction software to compensate for any motion experienced by the buoy while at sea. Both LiDARs delivered data points and average wind speeds based on a 10-min averaging period. The data provided by the LiDARs include mean wind speeds, wind speed variance, signal-to-noise ratio to assess quality, and direction at nine programable levels from 40–200 m above the system. Figure 3 shows the setup of a land-based measurement site, positioned at the Southern tip of the island, roughly 1.2 km east from the deployment site of the DeepCLiDAR Buoy offshore and provided a clear and open area for the LiDAR to take measurements. The land-based LiDAR was positioned with a line-of-site to the LiDAR buoy with little obstruction. Additionally, surface level wind speed and wave data from an existing nearby UMaine buoy, E01, were also collected during this time [16]. This served as another reference point for the measurements and provided concurrent wave height data for the land-based LiDAR data discussed later.

Figure 4 shows the DeepCLiDAR deployed offshore south west of the Island. The water depth was roughly 95 m and is approximately 1.26 km from Monhegan Island. Due to the distance between Monhegan Island and Maine's coastline, the site offered an open-ocean environment generally upwind of the island. The buoy collected 30-min significant wave height, H_s, and peak period measurements, 1-min current speeds, and 1-min directional data offshore. The buoy collected data for approximately seven months. A summary of sea state conditions at the buoy site is presented in Table 3.

3.2 Estimates of Wind Shear Using a Mesoscale Model. Estimates of wind shear exponents at the site were also made using a mesoscale model and are presented in Table 8. The mesoscale model used is the mesoscale atmospheric simulation system (MASS1), which was run in a series of nested grids, with the innermost grid having a spatial resolution of 1.2 km. The microscale model (WindMap) further refined this output to a horizontal grid spacing of 50 m. The source of topographic data was the National

Table 2 Summary of data collected and used in this study

Station	Sensor type	Elevation above mean sea level	Latitude and longitude (DD MM)	Date range	Average sampling period
Offshore, UMaine DeepCLiDAR Buoy	Wave	Surface	43°45′22.8″N 69°20′21.0″W	2/19/2016–10/28/2016	30 min
	Wind speed LiDAR	40–200 m			10 min
Land-based, Monhegan Island	Wind speed LiDAR	40–200 m	43°45′29.7″N 69°19′19.1″W	3/18/2014–7/21/2014 11/26/2015–04/19/2017	10 min
Offshore, reference buoy E01	Wave	Surface	43°42′53.4″N 69°21′18.0″W	7/9/2001–6/29/2017	30 min

Fig. 3 View of land-based LiDAR from north/northeast looking south/southwest over Lobster Cove, Monhegan Island

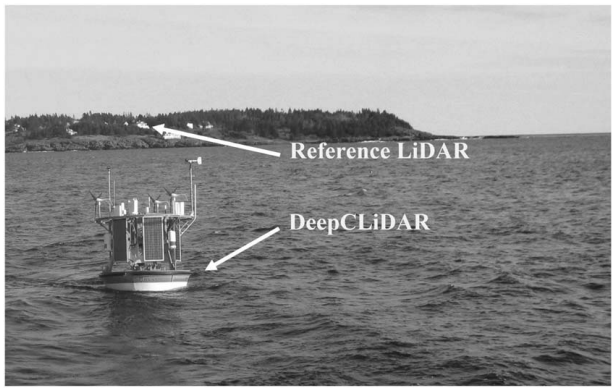

Fig. 4 View looking north of the DeepCLiDAR buoy system

Elevation Dataset, a digital terrain model produced on a 30 m grid by the US Geological Survey (USGS). The source of land cover data was the 30 m resolution National Land Cover Dataset, which is produced by the USGS and derived from Landsat imagery. While the majority of the mapped study area is open water, the land cover and topographic data were necessary to properly characterize wind flows over land features like Monhegan Island. In converting from land cover to surface roughness, the onshore roughness length values that were applied are believed to be typical of conditions in coastal Maine. However, the roughness could vary a good deal within each onshore class, potentially affecting the wind in the near shore environments.

The predictions of the model are compared to the measured average 10-min wind shear measured by the land-based and offshore LiDARs. In general, the measured wind shear is noticeably higher than the model predictions. The model was used to predict the monthly average wind shear exponent. The model estimates the wind shear for each hour of the day for each month. The values reported here are the average of the hourly average wind shear exponent predicted by the model for each day. The data show a difference in mean wind shear throughout the year ranging from 0.05 to 0.19. Summer months exhibit the highest wind shear while winter typically experiences lower wind shear values.

Table 3 Campaign average and maximum 30-min significant and maximum wave heights

Measurement	Average (m)	Maximum (m)	Average wave peak period (s)
H_s	1.04	5.30	9.5
Maximum wave height	1.73	8.94	

3.3 Wind Turbulence Intensity Measurements. Industry confidence in TI values calculated using LiDAR measurements is not typically accepted. While turbulence characteristics of atmospheric flows can be derived from LiDAR measurements, it is not nearly as established other methods [17]. When using vertical profilers, such as LiDAR, turbulence measurements generally experience two sources of difference from traditional measurements of TI. Variance is reduced due to the volumetric averaging of radial velocity measurements. Furthermore, variance is also effected by the cross contamination due to the scanning geometry of the LiDAR [18]. Issues with variance from a Windcube LiDAR specifically have been observed in a comparison of multi-LiDAR methods of measuring turbulence. Unstable conditions further showed variance contamination in horizontal measurements from the Windcube when compared to the multi-LiDAR setups [19]. Although the use of LiDAR for turbulence has known limitations, the data collected here are useful given that little if any turbulence data offshore the northeast US exists in the public domain. In this study, the TI was calculated directly from the LiDAR.

4 Results

4.1 LiDAR Measurements. Table 4 summaries the basic wind measurements made by the land-based LiDAR and DeepCLiDAR. The mean and STD of the 10-min wind speed measurements are presented for each LiDAR using all data screened based on "data availability" for each 10-min record at 40 m and 100 m above the sea level. Data availability is determined by the carrier-to-noise ratio and helps flag low signal strength, primarily due to insufficient particles in the air or other obstructions, which leads to inaccurate measurements. This is a standard practice among LiDAR measurements in the wind industry and helps lead to higher quality data collection and analysis. Because the land-based measurement record is longer than the DeepCLiDAR measurement record, concurrent land-based LiDAR measurements are also provided to facilitate comparison of the two datasets. These values are displayed in parentheses below the full data values.

4.2 Measured Wind Shear Exponents. Tables 5–7 show the measured wind shear values broken down into 2 m/s bins for all the land-based measurements, concurrent land-based measurements, and the offshore buoy measurements, respectively. Table 6 presents only the contemporaneous data measured by the land-based LiDAR

Table 4 Summary of wind speed measurements taken by LiDAR systems on land and offshore (land-based data collected at the same time as the offshore data are provided in parentheses)

	Land-based LiDAR		Offshore DeepCLiDAR	
Measurement	Mean (m/s)	STD (m/s)	Mean (m/s)	STD (m/s)
40 m wind speed: all data	7.73 (7.28)	3.62 (3.68)	7.64	3.86
40 m wind speed: availability >90%	7.58 (7.35)	3.65 (3.63)	7.68	3.85
100 m wind speed: all data	8.96 (9.11)	4.40 (4.78)	9.21	4.62
100 m wind speed: availability >90%	9.00 (9.24)	4.52 (4.76)	9.35	4.82

Table 5 Land-based reference LiDAR measured wind shear exponent α (all data are considered)

Wind speed bins (m/s)	Mean	STD	10th percentile	90th percentile	Number of data points
1–3	−0.05	0.52	−0.70	0.57	1722
3–5	0.12	0.33	−0.24	0.51	2814
5–7	0.19	0.22	−0.04	0.48	3875
7–9	0.23	0.20	0.02	0.50	3909
9–11	0.25	0.18	0.03	0.49	3519
11–13	0.26	0.18	0.04	0.47	2776
13–15	0.24	0.15	0.04	0.42	2153
15–17	0.25	0.13	0.05	0.41	1716
17–19	0.27	0.12	0.08	0.41	913
19–21	0.28	0.11	0.13	0.39	210
21–23	0.30	0.10	0.19	0.46	251
23–25	0.27	0.09	0.17	0.35	136
25–27	0.20	0.04	0.15	0.24	66
All data	0.20	0.28	−0.03	0.24	24,281

Table 6 Land-based reference LiDAR measured wind shear exponent α (only concurrent measurements with offshore LiDAR are considered)

Wind speed bins (m/s)	Mean	STD	10th percentile	90th percentile	Number of data points
1–3	−0.09	0.57	−0.76	0.63	1284
3–5	0.14	0.38	−0.29	0.59	2023
5–7	0.22	0.25	−0.08	0.53	2702
7–9	0.27	0.20	0.03	0.52	2837
9–11	0.30	0.18	0.09	0.53	2585
11–13	0.30	0.17	0.10	0.51	2048
13–15	0.28	0.16	0.06	0.46	1434
15–17	0.29	0.13	0.07	0.44	1126
17–19	0.31	0.10	0.15	0.42	631
19–21	0.30	0.10	0.15	0.41	153
21–23	0.32	0.10	0.21	0.47	189
23–25	0.29	0.09	0.19	0.43	97
25–27	0.20	0.04	0.15	0.26	32
All data	0.23	0.31	−0.08	0.51	17,306

for the purposes of comparing with the offshore LiDAR measurements. Statistical data are provided for each bin. Both of the two LiDAR measurement campaigns were generated over 24,000 10-min wind speed samples (over 167 days). The final row includes data below 1 m/s and above 27 m/s and therefore additional 221 and 271 data points are included. As expected, based on the annual wind speed distribution, not all of the wind speed bins have an equal amount of data. For both the land-based and DeepCLiDAR measurements, about 90% of the data occurs when the average wind speed is below 17 m/s.

Table 7 DeepCLiDAR measured wind shear exponent, α

Wind speed bins (m/s)	Mean	STD	10th percentile	90th percentile	Number of data points
1–3	−0.07	0.48	−0.66	0.58	2120
3–5	0.10	0.35	−0.26	0.53	3429
5–7	0.15	0.24	−0.08	0.47	4521
7–9	0.17	0.20	−0.03	0.43	5036
9–11	0.20	0.18	0.01	0.43	4450
11–13	0.21	0.16	0.03	0.41	3460
13–15	0.21	0.14	0.03	0.38	2167
15–17	0.24	0.12	0.04	0.38	1700
17–19	0.26	0.11	0.07	0.38	882
19–21	0.27	0.09	0.16	0.36	287
21–23	0.29	0.09	0.16	0.44	207
23–25	0.25	0.08	0.15	0.33	91
25–27	0.21	0.05	0.13	0.25	7
All data	0.15	0.27	−0.09	0.42	28,628

The data show a wide range of mean wind shear values for the different wind speed bins and significant variation within each bin as indicated by the STD and 10th/90th percentile values. The lower wind speed bins have low wind shear exponents and the exponent generally increases with the average 10-min wind speed bin. For the lowest wind speed bin of 1–3 m/s, the wind shear exponent is highly variable and the mean is negative. About 13% of the land-based and 19% of the LiDAR buoy wind shear exponent data were negative. However, these speeds are typically not too relevant for design of offshore wind systems since the cut in speed for most turbines is 4 m/s. The average wind shear exponent for wind speed bins above 11 m/s falls above 0.26 and 0.21 for the land-based and DeepCLiDAR datasets, respectively. These values are higher than the recommended industry standards in Table 1. The overall average wind shear exponent using the contemporaneous data for the land-based and DeepCLiDAR buoy are 0.20 and 0.15. Figures 5–7 present a scatter diagram of the measured wind shear exponents for the land-based and buoy LiDAR measurements versus 10-min mean wind speed at 100 m above mean sea level. The mean wind shear exponent for each 2 m/s bin and the 10th and 90th percentile for each bin are also plotted. The data show an increase in wind shear exponent as wind speed increases, up until roughly 24 m/s; however, it is unclear whether this drop is due to a physical phenomenon or due to a lack of data measurements at these higher wind speeds.

Table 8 Mesoscale model predicted wind shear exponents

Month	Average wind shear exponent, α		
	Mesoscale model	Reference LiDAR measurements	DeepCLiDAR measurements, α
Jan	0.05	0.12	NA
Feb	0.06	0.16	0.13
Mar	0.10	0.22	0.09
Apr	0.14	0.24	0.13
May	0.17	0.26	0.15
Jun	0.18	0.22	0.18
Jul	0.19	0.23	0.19
Aug	0.18	0.25	0.22
Sept	0.16	0.08	0.13
Oct	0.11	0.24	0.13
Nov	0.08	0.17	NA
Dec	0.06	0.12	NA
Yearly average	0.12	0.20	0.15

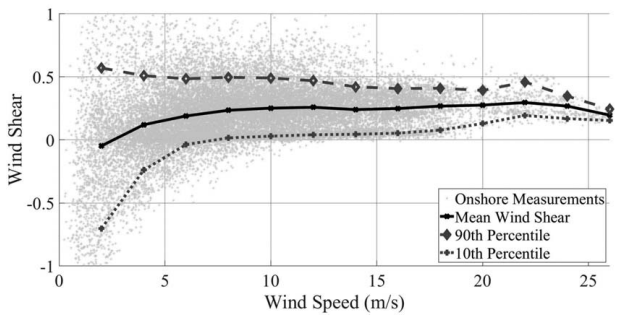

Fig. 5 Reference land-based LiDAR measured wind shear exponent versus 100 m wind speed data for all data. The mean wind shear exponent for each 2 m/s bin and the 10th and 90th percentile for each bin are plotted.

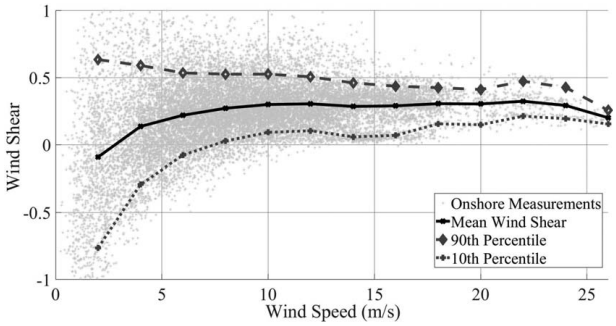

Fig. 6 Reference land-based LiDAR measured wind shear exponent versus 100 m wind speed data for contemporaneous data only. The mean wind shear exponent for each 2 m/s bin and the 10th and 90th percentile for each bin are plotted.

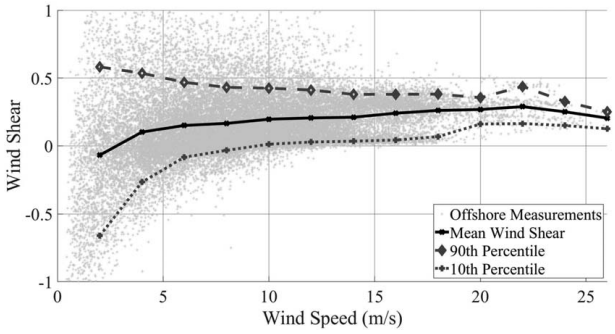

Fig. 7 Offshore DeepCLiDAR measured wind shear exponent versus 100 m wind speed with data. The mean wind shear exponent for each 2 m/s bin and the 10th and 90th percentile for each bin are plotted.

4.3 Wind Turbulence Intensity Measurements. Tables 9–11 present the TI data made from the land-based and DeepCLiDAR wind speed measurements at 100 m. When considering the concurrent data, the onshore LiDAR generally showed smaller TI for all wind speeds. This is possibly due to the motion of the buoy, although there is motion correction applied to the measurements by the manufacturer. Additionally, the difference could also be due to the geographical location and topography of the two sites.

Table 9 Land-based reference LiDAR wind TI at 100 m using all data

Wind speed bins (m/s)	Mean	STD	10th percentile	90th percentile	Number of data points
1–3	0.265	0.136	0.111	0.455	1722
3–5	0.139	0.067	0.057	0.225	2815
5–7	0.098	0.043	0.044	0.154	3878
7–9	0.077	0.036	0.033	0.126	3909
9–11	0.063	0.032	0.023	0.103	3519
11–13	0.056	0.027	0.021	0.090	2776
13–15	0.055	0.026	0.020	0.087	2153
15–17	0.045	0.021	0.017	0.074	1716
17–19	0.037	0.019	0.014	0.063	913
19–21	0.042	0.013	0.025	0.058	210
21–23	0.041	0.011	0.029	0.053	251
23–25	0.041	0.010	0.030	0.053	136
25–27	0.047	0.007	0.041	0.054	66
All data	0.093	0.085	0.026	0.174	24,285

Table 10 Land-based reference LiDAR wind TI at 100 m using contemporaneous data

Wind speed bins (m/s)	Mean	STD	10th percentile	90th percentile	Number of data points
1–3	0.235	0.129	0.098	0.422	1284
3–5	0.117	0.062	0.050	0.191	2024
5–7	0.082	0.039	0.039	0.131	2705
7–9	0.064	0.032	0.029	0.106	2837
9–11	0.052	0.029	0.021	0.087	2585
11–13	0.048	0.025	0.018	0.081	2048
13–15	0.045	0.025	0.018	0.076	1434
15–17	0.037	0.021	0.015	0.067	1126
17–19	0.030	0.017	0.013	0.056	631
19–21	0.039	0.013	0.016	0.058	153
21–23	0.039	0.011	0.029	0.050	189
23–25	0.039	0.009	0.030	0.048	97
25–27	0.045	0.005	0.038	0.052	32
All data	0.080	0.078	0.022	0.090	17,310

5 Discussion: Comparison of Data With Industry Design Guides

A comparison of the measured wind shear exponents against industry recommended design values is now presented. Table 12 presents a comparison of the measured exponents from the two LiDARs against industry design standards, the mesoscale model estimates, and a previous study.

The American Petroleum Institute (API) estimates for power law exponent and log profile roughness parameter were calculated following standard APR RP 2MET [20] for a 1-h wind speed of 20 m/s and converted to a 10-min mean wind speed. The API logarithmic wind shear model is different from the DNV model. The one-year mean wind speed at 4 m above sea level is equal to 21.4 m/s at the location of this experiment which, when converted to 1-h averaging period, is equivalent to 20 m/s. This wind speed was used for the purposes of comparison of the values estimated here. An equivalent roughness coefficient and wind shear exponent were calculated between 40 m and 100 m elevations for the purposes of comparing with the other standards. The API model is representative of offshore conditions, in strong, nearly neutrally stable atmospheric wind conditions during storms.

Several wind shear parameters are presented for each dataset and industry standard when available based on the roughness of the sea surface, which is characterized by the H_s conditions. The DeepCLiDAR buoy provides both wind and wave measurement instrumentation, which allows for the data to be screened and a separate mean

Table 11 Offfshore DeepCLiDAR measured wind TI at 100 m

Wind speed bins (m/s)	Mean	STD	10th percentile	90th percentile	Number of data points
1–3	0.252	0.111	0.228	0.408	2127
3–5	0.138	0.063	0.124	0.209	3434
5–7	0.103	0.042	0.095	0.157	4523
7–9	0.091	0.037	0.085	0.142	5036
9–11	0.083	0.036	0.076	0.131	4450
11–13	0.081	0.032	0.076	0.126	3460
13–15	0.083	0.030	0.079	0.123	2167
15–17	0.082	0.028	0.077	0.121	1700
17–19	0.080	0.026	0.079	0.117	882
19–21	0.094	0.021	0.090	0.118	287
21–23	0.091	0.015	0.089	0.113	207
23–25	0.091	0.014	0.090	0.108	91
25–27	0.095	0.007	0.091	0.103	7
All data	0.110	0.075	0.050	0.176	28,642

Table 12 Coastal wave environment and its relation to wind shear exponent and roughness coefficients for several standards and data collected in this study

Source	Terrain type	α, wind shear exponent	Z_0, wind shear roughness coefficient
Land-based LiDAR measurements	Coastal area with small waves (<1 m)	0.20	0.190
	Coastal area with medium waves ($1 < H_s < 3$ m)	0.19	0.144
	Coastal area with large waves ($H_s > 3$ m)	0.20	0.190
	All data	0.20	0.190
Offshore DeepCLiDAR buoy measurements	Open sea with small waves (<1 m)	0.14	0.023
	Open sea with medium waves ($1 < H_s < 3$ m)	0.18	0.108
	Open sea with large waves ($H_s > 3$ m)	0.19	0.144
	All data	0.15	0.035
DNV-RP-C205	Offshore without waves	0.07	0.0001
	Offshore with large waves	0.07	0.010
	Coastal areas with onshore wind (low)	0.11	0.001
	Coastal areas with onshore wind (high)	0.09	0.010
ABS	Offshore-normal winds	0.14	0.036
	Offshore-extreme winds	0.11	0.003
API RP 2MET	20 m/s wind speed at 10 m above sea level	0.08	0.0004
IEC 61400-3	Offshore-normal winds	0.20	0.190
	Offshore-extreme winds	0.20	0.190
ASCE-7	Offshore-annual average	0.16	0.054
Viselli et al.	Offshore-annual average	0.12	0.120
Mesoscale model	Annual average	0.12	0.009

wind shear to be reported for different H_s ranges. In this study, waves were considered to be low, medium, or large to be below 1 m, between 1 m and 3 m, or above 3 m H_s, respectively. The majority of the waves were classified as low: 62% low, 36% medium, and 2% large. The land-based LiDAR was similarly treated except concurrent H_s data were taken from the other nearby reference buoy, E01. E01 is roughly 5.5 km southwest from the land-based collection site. The majority of waves at E01 fall under 3 m: 46% low, 50% medium, and 4% large. These alternate wind shear values are presented and allow for comparison against industry standards, which provide typical wind shear values for different sea conditions.

DNV-RP-C205 presents a wide range of wind shear values for offshore and coastal conditions based on the wave conditions. The other standards do not present explicit wind shear conditions based on wave heights. ABS and IEC present a normal and extreme wind shear only. The normal wind shear is likely more typical of a low to medium wave environment and the extreme wind shear could be considered more close to the larger wave environmental conditions.

The offshore LiDAR average shear exponent of 0.15 exceeds the offshore DNV range of 0.08−0.13, the ABS values of 0.11−0.14, the previous study by Viselli et al., and the mesoscale model prediction. These data are less than both the 0.2 value recommended by IEC 61400-3 and the 0.16 value proposed by ASCE-7. As compared to API, the measured wind shear in the 19–21 m/s wind speed bin is equal to 0.27, which is significantly more than the API value.

The land-based LiDAR average shear exponent of 0.20 exceeds the offshore DNV range of 0.08−0.13, the ABS values of 0.11−0.14, the previous study by Viselli et al., and the mesoscale model prediction. These data match the 0.2 value recommended by IEC 61400-3 and exceeds the 0.16 value proposed by ASCE-7. As compared to API, the measured wind shear in the 19–21 m/s wind speed bin is equal to 0.28, which is significantly more than the API value.

Differences in these comparisons could be due to lack of multiple complete years of data as well as site specific conditions not specifically addressed by the standards and past studies. Differences in winds shear have been observed to be diurnal and seasonal, as shown in Table 8, and are due to "the stability of the atmosphere, which is governed by vertical temperature distribution from radiative heating or cooling of the earth's surface and the subsequent convective mixing of the air adjacent to the surface" [21]. This is especially true for offshore environments where there is a difference in sea and air temperature, which affects the lower boundary layer. Thus, wind speeds and therefore wind profiles are effected. Previous findings have shown that the stratification of the lower boundary layer is mainly unstable in the fall while stable in the spring [22].

The DeepCLiDAR was deployed for approximately 8 months from February to the end of October 2016. Considering the mesoscale model outputs, averaging this partial year dataset would tend to result in higher average wind shear considering that the majority of the winter months were not included in the average. This could explain the differences with the DNV, ABS, prior study, and the mesoscale model but would likely widen the gap against the IEC 61400-3 standard. The land-based LiDAR was deployed considerably longer for 21 months. However, the result of this additional data record is an increase in wind shear as compared to the offshore LiDAR, which is not expected based on the mesoscale model, which would expect a lower average wind shear to occur when more of the data from the winter months are

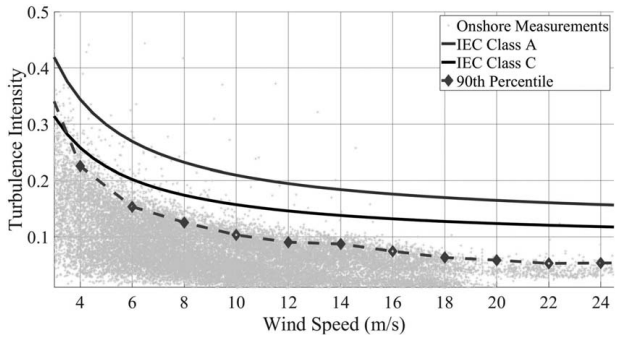

Fig. 8 Measured land-based wind TI versus 10-min mean wind speed at 100 m

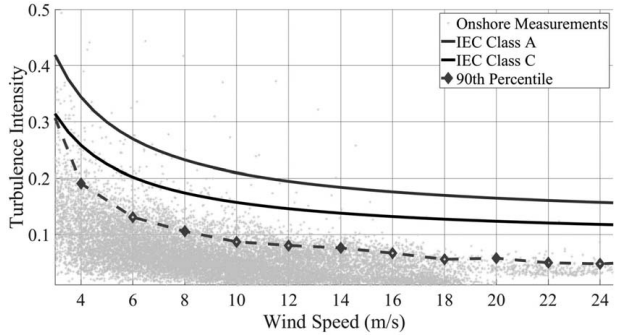

Fig. 9 Measured land-based wind TI versus 10-min mean wind speed at 100 m using concurrent data

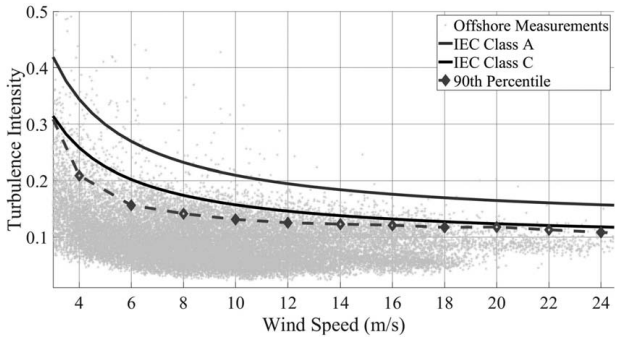

Fig. 10 Measured offshore wind TI versus 10-min mean wind speed at 100 m

considered. When considering specific data points, considerably more deviation from the standards exists. The spread on the data for wind shear is highly variable and the values can increase or decrease significantly from the reported averages. In some cases, a negative wind shear occurs, which is not well discussed in current offshore standards. This dataset includes a number of negative wind shear values as mentioned.

A comparison of the measured TI against IEC standards is now presented. Figures 8–10 present the measured turbulence from the land-based LiDAR and DeepCLiDAR. In addition to the measured data, the 90% percentile/quantile of the measurements is provided for comparison against the IEC 61400-1 industry turbulence class TI curves for class A and class C site conditions. The land-based and DeepCLiDAR 90% quantiles fall below the class C curve for all wind speed bins above about 2 m/s.

6 Summary and Conclusions

A unique high-altitude (40–200 m) wind speed dataset has been analyzed and provided in this paper. The data were collected in the Northeast USA in support of the development of the first floating offshore wind project in the USA planned for grid-connection by 2023. There is currently a lack of wind speed data at high altitudes in the USA making these first measurements useful for understanding the wind conditions offshore in the USA for future research and wind developments. This testing campaign consisted of two LiDAR wind measurement devices collecting data simultaneously. One was positioned on land and other offshore on a DeepCLiDAR buoy.

The data from this campaign suggest that wind shear varies throughout the year with wind speed and for different wave conditions. The mean measured wind shears exceeded those presented in most industry recommendations. It was not uncommon to see a wind shear exponent above 0.20 with wind speeds above 10 m/s. Industry standards generally present only a one or two representative wind shear values for all design load cases. In reality, wind shear varies significantly. Higher wind shear could have an impact on the loading of the offshore wind system. For example, the loading on the blade will vary more with increased wind shear as it rotates through a larger variation of wind speed.

Both onshore and offshore LiDAR wind turbulence measurements are not currently used as a reliable measurement. The data are presented in this paper because there is little offshore turbulence measurements available in the USA. The data show that the offshore wind turbulence at 100 m was below IEC 61400-1 class C.

In summary, these data campaigns and analysis suggest that wind shear may need to be considered carefully given the significant variation possible and the higher mean values recorded as compared to recommended industry values recommend for design of wind energy systems. Additional long-term offshore wind data collection campaigns would help to confirm these findings and determine if these trends are typical for other regions in the Northeast USA.

Acknowledgment

The authors would like to acknowledge the support of the US Department of Energy Office of Energy Efficiency and Renewable Energy (Grant Numbers DE-EE0005990 and DE-EE0006713), the State of Maine 2010 State Bond, the Maine Technology Institute (Grant Number DL-4006), the Rockefeller Brothers, the Davis Family Foundation, the University of Maine, the University of Maine Physical Oceanography Group, NRG Renewables, and AWS Truepower-UL.

Nomenclature

u = wind speed (m/s)
z = height (m)
H = height (m)
H = reference height above sea level
u_r = reference or measured wind speed (m/s)
z_r = reference height (m)
z_0 = logarithmic wind shear law roughness parameter (m)
H_s = significant wave height (m)
u' = root-mean-square of velocity fluctuation (STD)
hub-height = height of wind turbine rotor center above mean sea level (m)
uX = wind speed (m/s) at height X (m)
α = wind shear power law exponent

References

[1] Newman, R., 2016, *Optimizing Lidar Wind Measurements From the DOE WindSentinel Buoys*, Pacific Northwest National Laboratory, Richland, WA.

[2] Schwartz, M., Heimiller, D., Haymes, S., and Musial, W., 2010, *Assessment of Offshore Wind Energy Resources for the United States*, National Renewable Energy Laboratory, Golden, CO.

[3] AWS Truewind, LLC, 2010, *New York's Offshore Wind Energy Development Potential in the Great Lakes: Feasibility Study*, Albany, NY.

[4] Viselli, A., Forristall, G., Pearce, B., and Dagher, H., 2015, "Estimation of Extreme Wave and Wind Design Parameters for Offshore Wind Turbines in the Gulf of Maine Using a POT Method," Ocean Eng., **104**, pp. 649–658.

[5] Pichugina, Y. L., Banta, R. M., Brewer, W. A., Sandberg, S. P., and Hardesty, R. M., 2012, "Doppler Lidar-Based Wind-Profile Measurement System for Offshore Wind-Energy and Other Marine Boundary Layer Applications," J. Appl. Meteorol. Climatol., **51**(2), pp. 327–349.

[6] Lange, B., Larsen, S., Højstrup, J., and Barthelmie, R. J., 2004, "Importance of Thermal Effects and Sea Surface Roughness for Wind Resource and Wind Shear at Offshore Sites," Wind Eng. Ind. Aerodyn., **92**(9), pp. 959–988.

[7] Pena Diaz, A., Gryning, S.-E., Mikkelsen, T. K., Hasager, C. B., and Kelly, M. C., 2012, "The Modeling and Observation of the Long-Term Vertical Wind Profile and Wind Shear," Proceedings of EWEA 2012—European Wind Energy Conference & Exhibition European Wind Energy Association (EWEA), Copenhagen, Denmark, Apr. 16–19.

[8] Pena Diaz, A., Mikkelsen, T. K., Gryning, S.-E., Hasager, C. B., Hahmann, A. N., Badger, M., Karagali, I., and Courtney, M., 2012, "Offshore Vertical Wind Shear:

Final Report on NORSEWInD's Work Task 3.1," DTU Wind Energy, Kongens Lyngby, Denmark.
[9] DNV, 2010, *DNV-RP-C205—Environmental Conditions and Environmental Loads*, Det Norske Veritas, Oslo.
[10] IEC, 2009, *International Standard IEC 61400-03*, 1st ed., International Electrotechnical Commission, Geneva.
[11] Øistad, I. S., 2015, *Analysis of the Turbulence Intensity at Skipheia Measurement Station*, Norwegian University of Science and Technology, Trondheim.
[12] Argyle, P., Watson, S., Montavon, C., Jones, I., and Smith, M., 2015, *Turbulence Intensity Within Large Offshore Wind Farms*, European Wind Energy Association, Paris.
[13] ABS, 2020, *Guide for Building and Classing Floating Offshore Wind Turbine Installations*, American Bureau of Shipping, Houston, TX.
[14] ASCE, 2010, *Minimum Design Loads for Buildings and Other Structures*, American Society of Civil Engineers, Reston, VA.
[15] Viselli, A., Filippelli, M., Pettigrew, N., and Dagher, H., 2018, "Validation of a LiDAR Wind Resource Assessment Buoy System in US Northeast Waters Against a Fixed Land-Based LiDAR System," Wind Energy J., **22**, pp. 1548–1562.
[16] Pettigrew, N., Xue, H., Irish, J., Perrie, W., Roesler, C., Thomas, A., and Townsend, D., 2008, "The Gulf of Maine Ocean Observing System: Generic Lessons Learned in the First Seven Years of Operation (2001–2008)," MTS J., **43**(3), pp. 91–102.
[17] Sathe, A., Mann, J., Vasiljevic, N., and Lea, G., 2015, "A Six-Beam Method to Measure Turbulence Statistics Using Ground-Based Wind LiDARS," Atmos. Meas. Technol., **8**(2), pp. 729–740.
[18] Sathe, A., Mann, J., Gottschall, J., and Courtney, M., 2011, "Can Wind LiDARs Measure Turbulence?," J. Atmos. Ocean Technol., **28**(7), pp. 853–868.
[19] Newman, J. F., Bonin, T. A., Klein, P. M., Wharton, S., and Newsom, R. K., 2016, "Testing and Validation of Multi-LiDAR Scanning Strategies for Wind Energy Applications," Wind Energy J., **19**(12), pp. 2239–2254.
[20] American Petroleum Institute, 2014, *Derivation of Metocean Design and Operating Conditions*, API Publishing Services, Washington, DC.
[21] Spera, David, PhD, 2009, *Wind Turbine Technology Fundamental Concepts of Wind Turbine Engineering*, 2nd ed., ASME, New York, pp. 488–492.
[22] Van Wijk, A. J. M., Beljaars, A. C. M., Holtslag, A. A. M., and Turkenburg, W. C., 1990, "Evaluation of Stability Corrections in Wind Speed Profiles Over the North Sea," J. Wind Eng. Ind. Aerodyn., **33**(3), pp. 551–566.